RSC Advances

ROYAL SOCIETY OF CHEMISTRY

www.rsc.org/advances

Journal Name

RSCPublishing

ARTICLE

Discovery of NAD(P)H:quinone oxidoreductase 1 (NQO1) inhibitors with novel chemical scaffolds by shape-based virtual screening combined with cascade docking

Cite this: DOI: 10.1039/x0xx00000x

Received 00th January 2012,
Accepted 00th January 2012

DOI: 10.1039/x0xx00000x

www.rsc.org/

Jinlei Bian, [a,c] Xue Qian, [a,c] Bang Deng, [a,c] Xiaoli Xu, [a,c] Xiaoke Guo, [a,c] Yalou Wang, [a,c,*] Xiang Li, [a,c] Haopeng Sun, [a,c] Qidong You [a,b,c,*] and Xiaojin Zhang [a,d,*]

A number of novel NAD(P)H:quinone oxidoreductase 1 (NQO1) inhibitors were discovered from the ChmeDiv database via a simple protocol. Based on two reference NQO1 inhibitors, dicoumarol (DIC) and ES936, shape-based similarity search and cascade docking filtering were conducted to identify new NQO1 inhibitors. Using these techniques, 43 compounds were selected, ordered, and tested. Among them, 7 compounds with novel chemical scaffolds were confirmed to be active by in vitro assays. Determination of the ability for protecting against NQO1-mediated toxicity of β-lapachone (β-lap) confirmed that compounds **8**, **10** and **13** may be pharmacological useful for probing the function of NQO1 in cells.

1. Introduction

NAD(P)H:quinone oxidoreductase-1 (NQO1, DT-diaphorase) is a ubiquitous flavoprotein that is widely distributed in animals, plants, and bacteria.[1] It has been shown that NQO1 has a molecular weight of about 60 kDa, and is a homodimer of two interlocked monomers of 274 amino acids.[2] Each subunit is composed by two domains, a catalytic domain (residues 1-220) and a C-terminal domain that forms part of the binding site for the hydrophilic regions of NAD(P)H.[3,4] The active site of human NQO1 is located at the interface of the two monomer units. The catalytic site can be divided into three regions: the FAD binding site, the hydrophilic adenine-ribose portion of NAD(P)H binds and the site occupied by the cofactor (the hydride donor) or the substrate (the hydride acceptor).[5] The catalytic cycle of NQO1 functions via a ping-pong mechanism in two steps, NAD(P)H binds to NQO1, reduces the FAD cofactor to $FADH_2$ and is then released in its oxidized form $NAD(P)^+$, allowing the quinone substrate to bind to the enzyme and to be reduced by $FADH_2$.[6]

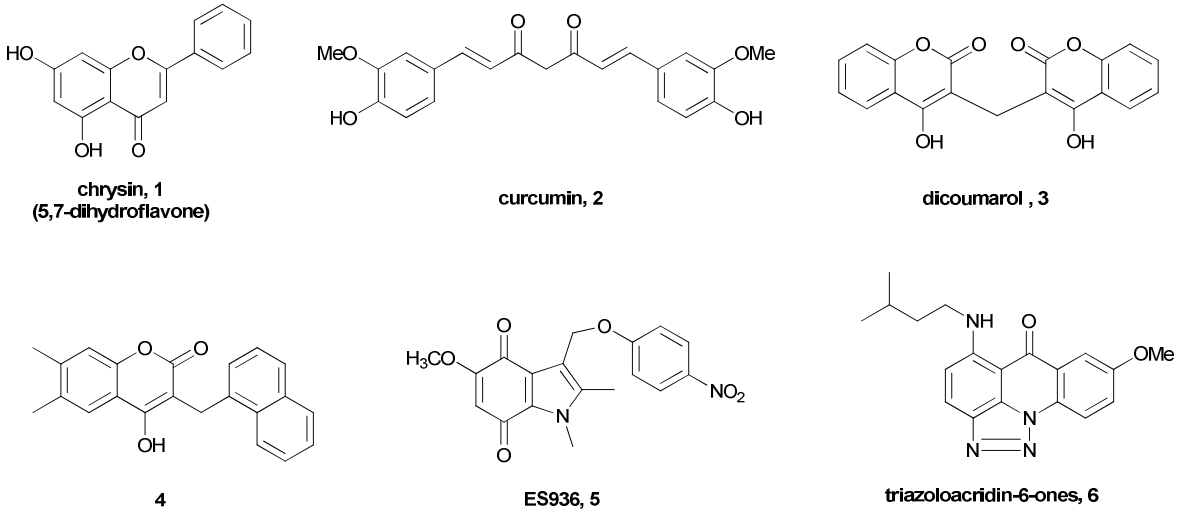

Fig. 1 Representative structures of known inhibitors of NQO1.

Journal Name RSCPublishing

ARTICLE

Typically, NQO1 can reduce quinones, forming stable hydroquinones. Glutathione S-transferase then detoxifies hydroquinones, conjugating them with glutathione for secretion.[7] However, NQO1 is also involved in the reductive activation of anticancer agents, such as mitomycin C (MMC), EO9, RH1, streptonigrin (STN), lavendamycin, deoxynyboquinone (DNQ), and β-lapachone (β-lap) that operate by the so-called bioreductive mechanism, and continues to generate interest because of its dramatic elevation in many solid tumors.[8] An additional function of NQO1 is its ability to act as a chaperone protein. It has been believed to be a gatekeeper of the 20S proteasome pathway and plays an important role in protecting the tumor suppressor protein p53 against proteosome degradation, which leads the stabilization and activation of p53.[9] Inhibition of NQO1 enzyme activity results in destabilization of p53 and similar NQO1-mediated effects have been observed for several other short-lived proteins including ornithine decarboxylase and proteins important in the regulation of mRNA translation.[10,11] A number of compounds are known to inhibit the activity of NQO1 by completing with NAD(P)H for binding to the enzyme thereby preventing reduction of the FAD (Fig. 1). These include a number of flavons, coumarins, curcumin and the triazoloacridin-6-ones, but the most representative inhibitors are dicoumarol (DIC) and ES936.[12,13] DIC and ES936 are frequently used to study the consequences of a lack of NQO1 function in cells, and many pharmacological studies of NQO1 rely on the use of these two inhibitors.[14,15] In particular, it is important to emphasize that ES936 is the mechanism-based suicide inhibitor which is different with the competitive inhibitors such as DIC.[13] Efficient inhibitors of NQO1 could be widely used in studies of NQO1-mediated cell death and identify the importance of NQO1 for determining protein stability.[6,9] Thus, in order to better understand the pharmacological function of NQO1, some new scaffolds of NQO1 inhibitors are urgent to develop.

There were some studies on the discovery of new NQO1 inhibitors,[10,16-18] mainly focused on DIC (**3**) and triazoloactidin-6-ones (**6**). Very few studies have been published about the identification of NQO1 inhibitory compounds by virtual screening (VS) methods. Besides, several crystals of NQO1 have been solved making a VS approach possible. Therefore, in this present work, we developed a ligand-based virtual screening using the ROCS (OpenEye Scientific Sofaware, Inc.) method[19] of molecular shape to obtain an enriched subset of the ChemDiv database[20] of commercially available screening compounds. We used DIC and ES936 as the template in a shape/electrostatic similarity analysis to identify compounds whose structures were consistent with NQO1 inhibitory activity. Compounds with higher similarity index with the reference means higher structural and functional group similarity. Such compounds were selected as candidates for the second round filtering, in which cascade docking and scoring were conducted against the candidate compounds. A diversity analysis was then undertaken using the program Diverse Subset (MOE 2013.08). Top 10% of the molecules were selected. Finally, 43 hit compounds were purchased from the ChemDiv for biological testing. Among them, 7 compounds exhibiting potent inhibition of NQO1 were selected. Determination of the ability for protecting against NQO1-mediated toxicity of β-lap confirmed that compounds **8**, **10** and **13** may be pharmacological useful for probing the function of NQO1 in cells. The VS method we reported here was useful to guide the researchers to efficaciously identify novel inhibitors for NQO1.

2. Methodology

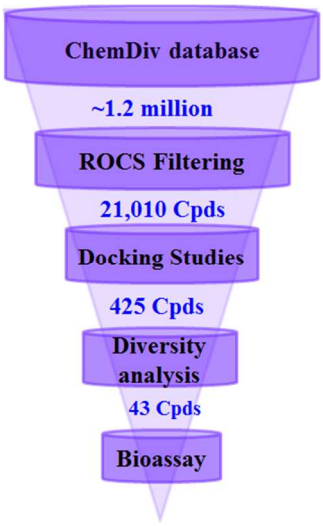

Fig. 2 shows the computational protocol that was applied to NQO1 inhibitors. Full details of each step are discussed in the following paragraphs.

2.1. Compound database preparation

A drug-like subset of the ChemDiv database of commercially available compounds was downloaded, and the bank of 1.2 million compounds was prepared with the module of Search Conformations in Molecular Operating Environment (MOE)[21] to provide an average of 137 conformations per compound. These structures were washed, i.e. all inorganic compounds were removed and all ionizable groups were set to coordinated with neutral pH conditions. Energetically minimized conformations were generated using the MMFF94x force field.

2.2. Shape-based virtual screening

ROCS is an acronym for 'Rapid overlay of Chemical Structures', a virtual screening application of OpenEye Scientific Software.[22] ROCS represents heavy atoms by Gaussians with parametrized decay constants according to the respective van der Walls radii. This representation of atoms allows a fast shape comparison of molecules due to the straightforward calculation of molecular overlaps providing sufficient speed for virtual screening of large databases.[23] Besides shape description ROCS includes a color force field allowing for basic inclusion of chemical information in the screening process which is called color score.[24] The color force fields in ROCS define six type force-field, including hydrogen-

bond donors, hydrogen-bond acceptors, hydrophobes, anions, cations, and rings. Combination of both scores results in the 'combo score', which was used for all screening reported in this work. Default settings were used for all screening runs.

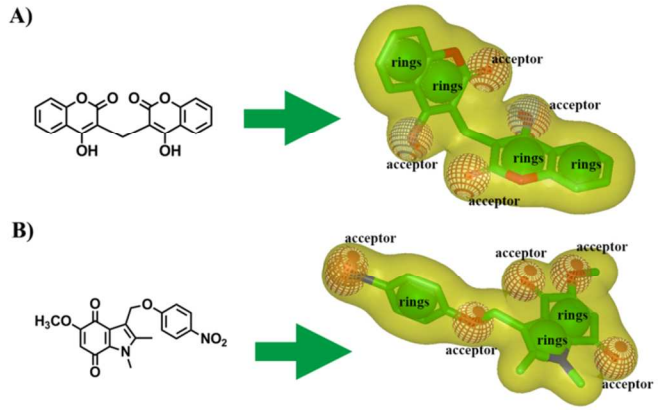

Fig. 3 ROCS shape query derived from a low energy 3D conformation generated in MOE 2013.08 of DIC and ES936. The green spheres illustrate ROCS ring features, and the red spheres illustrate hydrogen bond acceptors.

DIC and ES936 were selected as the reference molecule to generate the ROCS model. The structure of DIC and ES936 were separated from the cocrystal complex (PDB ID: 2F1O and 1KBQ) and further minimized using MOE with MMFF94x forcefield. Then the two molecules were directly used to generate the ROCS queries. The molecular shape of DIC and ES936 were depicted in a yellow surface (Fig. 3). The 3D similarity was ranked by two methods: The ShapeTanimoto and the ComboScore method which was consist of the shape Tanimoto coefficient.

In order to validate the reliability of the model, an active set including 18 compounds was collected from literature (SI, Table S1).[17-18] As a set of experimentally confirmed inactive compounds was not available, we used large databases as decoy sets to assess virtual screening efficiency. The decoy set was downloaded from Directory of Useful Decoys (DUD, http://dud.docking.org/) containing 375 compounds with similar physicochemical properties to DIC. A special note is that the decoy set was also employed in the docking work. Enrichment factors, receiver operating characteristic (ROC) curves, and areas under the ROC-curves (AUC) were used for screening quality assessment. The enrichment factor indicates the improvement of the hit rate achieved by a virtual screening approach compared to a random selection.[25] It is calculated as the ratio of actives in the hit list at a given percentage of the database. Enrichment factors at 1% were calculated for Fig. 4 to focus on the early enrichment. The ROC curve provides a graphic representation of the distribution of actives in a database of supposedly inactive compounds ranked by virtual screening.[26] The x-axis represents all molecules in a database rank-ordered by shape-based screening, scaled from 0 to 100%. For every active ligand in the rank-ordered list, the curve raises one step in the y-direction. A steep slope at the beginning of the curve therefore indicates a high enrichment of active ligands among the highest ranked molecules and therefore high screening success. A theoretically perfect performance would correspond to an area under the curve (AUC) value of 1.0, while a random performance gives an AUC value of 0.5. AUC values less than 0.5 represents an unfavorable case with a systematic ranking of decoys higher than the rankings of known actives. AUC values signify the discriminative capacity of the protocol, when database screened is plotted as a function against actives recovered.[24]

2.3. Cascade docking

2.3.1. Native-docking

The crystallographic coordinates of human NQO1-inhibitors (PDB code 2F1O, 3JSX, 1KBQ, 1KBO) were used to conduct native-docking. These ligands were docked back into their corresponding protein structures using Gold5.1 (CCDCs software GOLD version 5.1), Libdock, CDOCKER (DS 3.0), alpha PMI (Principal Moments of Inertia, MOE 2013.08) and Glide (Schrödinger 2009). To define the binding pocket of NQO1 cocrystal structure, residues around the native ligand (radius set as 8.0 Å) were selected for molecular docking. All other parameters are set as default. The docking results were evaluated through comparison of the best docked poses and the real cocrystallized pose to measure docking reliability. The best docked poses were defined as the pose returned that is closest to the crystal. The docking software with the smallest root mean square deviation (RMSD) would be picked to perform cross-docking.

2.3.2. Cross-docking

The complexes used in native-docking were also selected to perform cross-docking evaluation.[27] The native ligands were docked into all complex structures using the docking software confirmed by native-docking. The docking reliability was evaluated by calculating the RMSD difference of each ligand between the reference positions of the ligand in the experimental NQO1-ligand complex and positions predicted by the docking software. Finally the protein which had the smallest RMSD was selected as the working protein.

2.3.3. Docking with decoy

To validate the docking results, a decoy database was built. Besides, docking with decoys helps us determine the percentage of the ranked compounds that we should select in the cascade docking. The decoy database was used to validate the shape-based virtual screening previously carried out. The parameters of the docking function were determined by Native-Docking and Cross-Docking. The enrichment factor (EF) was calculated using the decoy database according to the following formula

$$EF = \frac{a/n}{A/N}$$

Where n = total number of hits, a = the total number of active molecules in the n hits, N = total number of molecules in database, and A = the total of actives in the database. The decoy database was built by mixing 18 active NQO1 inhibitors (Supporting Information, Table 1) with 42 inactive inhibitors (IC_{50} > 50 μmol•L^{-1}), and 375 compounds selected with similar physicochemical properties to DIC from DUD. All the compounds were converted to 3D structures using the 3D Conformation Search module in MOE software.

2.5. Biology

2.5.1 NQO1 Inhibition Studies

The compounds identified as possible NQO1 inhibitors were purchased from ChemDiv, Inc. The purchased compounds were assayed for their ability to inhibit the quinone reductase NQO1 employing purified recombinant human NQO1. For testing their binding affinities to NQO1 protein, we performed the assay using the following methods. Recombinant human NQO1 (DT-diaphorase, EC 1.6.5.5) was obtained from Sigma

and diluted in 50 mmol•L^{-1} phosphate buffer to give an enzyme activity that would result in a change in optical absorbance of substrate (β-lap) of approximately 0.1 per minute.[6] The enzyme reaction was started by adding 5 µL of this solution to 495 µL of 50 mmol•L^{-1} phosphate buffer at PH 7.4 containing 200 µmol•L^{-1} NADPH for NQO1, with 0.14% (w/v) BSA, together with various concentrations of the potential inhibitor dissolved in DMSO (final concentration 1.0% v/v). The DMSO concentration used was sufficiently small to ensure minimal perturbation of hydrogen bonding networks in aqueous NQO1 complexes. Reaction was initiated by automated dispensing of the NADPH solution into the wells, and data was recorded at 2 s intervals for 5 min at room temperature (22-25 °C). The oxidation of NADPH to NADP$^+$ was monitored at 340 nm on a Varioskan Flash (Thermo, Waltham, MA). Each measurement was made in triplicate and the experiments carried out three times. The IC_{50} curves were generated using Graphpad Prism 6.

2.5.2 Impact of NQO1 inhibition on β-lap toxicity in cells

Impact of NQO1 inhibition on β-lap toxicity was determined by the MTT assay. Cells were plated in 96-well plates at a density of 10,000 cells/mL and allowed to attach overnight (16 h). Cells were then given 30 µmol•L^{-1} DIC or the other compounds with various concentrations of β-lap for 2 h, removed, and replaced with fresh medium and the plates were incubated at 37 °C under a humidified atmosphere containing 5% CO_2 for 72 h. MTT was added and the cells were incubated for another 4 h. Medium/MTT solutions were removed carefully by aspiration, the MTT formazan crystals were dissolved in 100 µL of DMSO, and absorbance was determined on a plate at 540 nm. Values of IC_{50} were calculated as the concentration of β-lap, which in the presence of 30 µmol•L^{-1} inhibitors, cause 50% cell kill. All toxicity experiments were repeated on at least three technical replicates. Data were analysed and curves were generated using Graphpad Prism 6.

3. Results and discussion

3.1. Shape-based virtual screen

3.1.1. Validation of the screening protocol

To ensure the ability to discern true positives of the shape-based screening protocol, the in silico validation of our screening protocol was performed, beforehand. A decoy set was prepared from DUD containing 375 compounds with similar physicochemical properties to DIC. This ensures that enrichment calculations carried out from such data sets to be free of bias and accurate.[28]

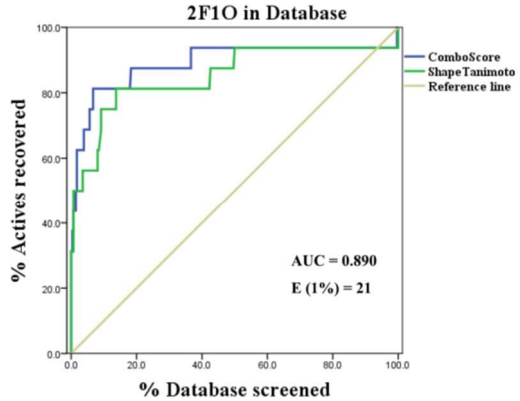

Fig. 4 ROC-curves for DIC screening the database. The comboscore (blue) outperforms pure shapescore (green). AUC and early enrichment (E) at 1% of the hit list are indicated for screening with comboscore

There are a number of methods to gauge the success of a screening tool. One commonly used measure that assesses the performance of a virtual screening strategy is the receiver operating characteristic (ROC) curve. DIC turned out to be a good query molecule. Using the 3D shape information together with the chemical information (Combo Score) of the ligand yielded an AUC value of 0.890 (see Fig. 4). To cover a range of the inhibitors sizes, ES936 (PDB code: 1KBQ) was also selected as query for ROCS screening runs. ES936 has a different chemical scaffold which is dissimilar to DIC in a ranking of all active ligands, and then a worse AUC was obtained (data not shown). Whereas ES936 is the most active mechanism-based suicide inhibitor of NQO1, it helps to recover some potent NQO1 inhibitors.

3.1.2. The result of shape-based virtual screen

The shape queries of DIC and ES936 were set to screen the ChemDiv database, containing approximately 1.2 million molecules. The top 1% of ranked compounds for both queries was carried forward for docking. It is important to note that there were really some overlapped molecules obtained from both queries.

3.2. Docking results

3.2.1. Comparison of the structures of hNQO1-substrates, hNQO1-inhibitors with Apo hNQO1

Eight hNQO1 structures with crystallographic resolution from 1.70 Å to 2.75 Å were utilized in this work. These structures can be divided into three groups, its native structure (PDB code 1D4A),[3] as well as its behavior with substrates, such as duroquinone (PDB code 1DXO), EO9 (PDB code 1GG5), CB1954 (PDB code 1QBG), and inhibitors, including DIC (PDB code 2F1O), AS1 (PDB code 3JSX), ES1340 (PDB code 1KBO), ES936 (PDB code 1KBQ).[3-5,10,18,29] To compare the backbone conformation, 1D4A was used as the reference and the other structure was superposed onto it, and the RMSD was calculated (varies from 0.36 to 0.74 RMS deviation for the α-carbon atoms, Fig. 5A). The low RMSD indicated that these NQO1 structures showed a high similarity. However, there is a significant movement of two residues (Tyr128 and Phe232) in the catalytic pocket of hNQO1-inhibitors compared to NQO1-substrates and Apo hNQO1 (Fig. 5B). In this study, we mainly focus our efforts on discovering new inhibitors of NQO1, and then the hNQO1-inhibitor crystal complexes (PDB code: 2F1O, 3JSX, 1KBO and 1KBQ) were selected to perform docking screening.

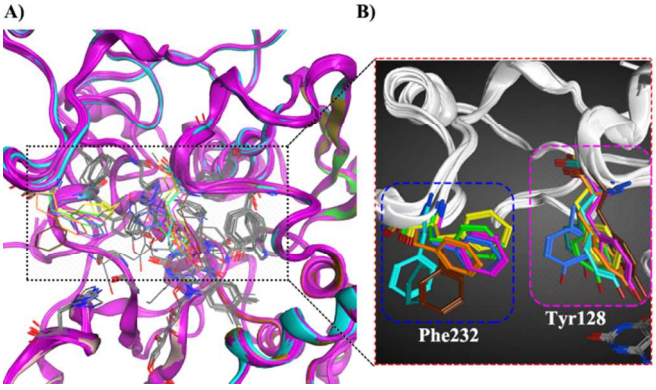

Fig. 5 (A) The superimposition of eight hNQO1 crystal structures. (B) The significant movement of two residues (Tyr128 and Phe232) in the catalytic pocket of hNQO1-inhibitors compared to NQO1-substrates and Apo hNQO1.

3.2.2. Cascade docking results

According to the results of Native-Docking of four NQO1-inhibitor ligands to their native proteins (Table 1), docking using the Gold5.1 software package with GoldScore scoring function had the smallest average RMSD and standard deviation (std). It indicated that Gold5.1 showed higher reproducibility than Libdock, CDOCKER, alpha PMI, and Glide programs. Therefore, we used the Gold5.1 to dock proteins with inhibitors. Referring to the result of Cross-Docking (Table 2), docking using 2F1O with various ligands had the smallest average RMSD (2.0) and std (0.81). For these reasons, Gold5.1 and 2F1O were selected to perform docking screening.

Table 1 RMSD of NQO1-inhibitor complexes used for native-docking

PDB (complex)	Docking Software				
	Gold5.1	Libdock	CDOCKER	alpha PMI	Glide
1KBO	0.8	2.1	1.7	2.1	1.8
1KBQ	1.5	2.8	2.3	3.0	2.1
2F1O	0.8	1.6	2.0	1.4	1.5
3JSX	1.1	2.3	0.9	2.2	1.3
av[a]	1.2	2.2	1.7	2.2	1.7
std[b]	0.28	0.43	0.52	0.57	0.30

[a]Average RMSD values of native ligand poses referring to their native poses. [b]Standard deviation of these RMSD values.

Table 2 RMSD of ligands in cross-docking using the Gold software

PDB (complex)	Native ligands extracted from complexes			
	ES1340	ES936	DIC	AS1
1KBO	0.8	4.1	3.1	4.0
1KBQ	4.0	4.1	2.0	3.9
2F1O	2.2	1.8	0.8	2.1
3JSX	2.5	3.1	2.2	1.9
av[a]	2.4	3.3	2.0	3.0
std[b]	1.13	0.94	0.81	0.98

[a]Average RMSD values of native ligand poses referring to their native poses. [b]Standard deviation of these RMSD values.

3.2.3. The results of molecular docking

After the previous virtual screening, the remaining compounds were submitted docking simulation using the genetic optimization for ligand docking (Gold5.1) software package. The binding site was defined as being any volume within 8 Å of the scaffold of DIC in its crystal pose in 2F1O, and the residues Trp105, Phe106, Tyr126, Tyr128, Gly149, Gly150, Met154, His161, His194, Phe232 and Phe236 were found to be interacting residues as shown in Fig. 6.

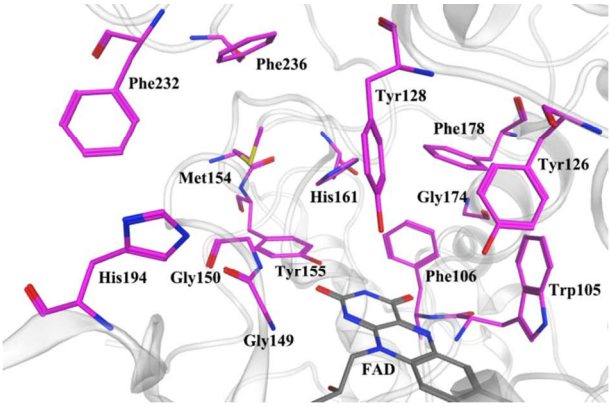

Fig. 6 The binding site of DIC with NQO1. The binding pattern was generated from the cocrystal structure (PDB code: 2F1O) depicted using MOE 2013.08. The carbon atoms of FAD and the key residues in the active site of NQO1 were colored in gray and purple, respectively.

Upon that, docking with decoys was used to select hits and evaluate the docking result. By calculating the EF value in different percent of top molecules ranked with score, we could know which percent of ranked molecules hit the active compounds and reduce the false positive. The EF value in 0.1%, 1%, 2% and 5% top ranked molecules were 1.2, 5.2, 7.9, and 1.0. For this reason, the best percent of ranked molecules to be selected was 2%. Thus, 2F1O was used as the working protein and Gold5.1 was employed as the docking program and 2% of the ranked molecules would remain. After cascade docking, 425 hits (2% of the ranked compounds) were obtained. 352 hits came from the query DIC, and others from the query ES936. Because this number included a large degree of similar compounds, with respect to scaffold and chemical class, a diversity analysis was undertaken using the program Diverse Subset (MOE 2013.08). Top 10% of the molecules were selected.

Journal Name RSCPublishing

ARTICLE

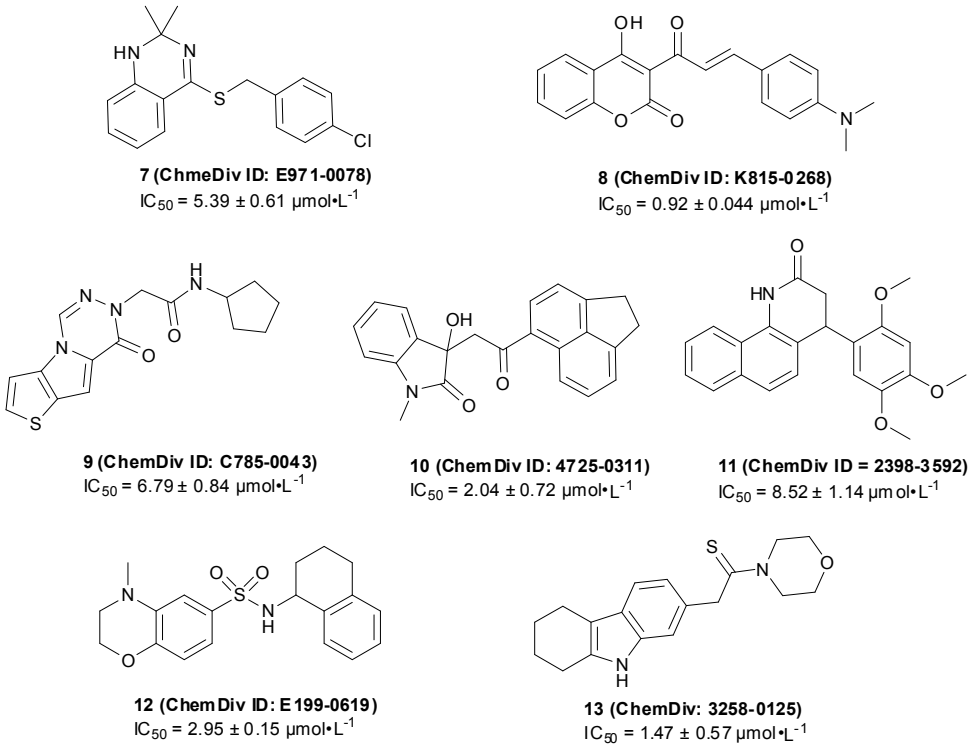

Fig. 7 Seven ligands were found by VS from the database.

3.4. Biological evaluation of the hit compounds

Finally, 43 novel compounds with diverse scaffolds were selected for testing their ability to inhibit recombinant hNQO1 in vitro. All of these compounds were assayed in the presence of 0.14% (w/v) BSA, considering the effect of nonspecific protein binding. Based on the assay, seven compounds (**7** to **13**) revealed potential inhibitory activity to NQO1 (Fig. 7). Most of the compounds had a high degree of dissimilarity to each other, and possessed novel scaffolds with respect to the known active inhibitors. Among the seven active compounds, **8** had the highest binding affinity with IC_{50} value of 0.92 ± 0.044 μmol•L^{-1}. Comparing **8** to the recognized NQO1 inhibitor, DIC had IC_{50} value of 0.30 ± 0.081 μmol•L^{-1} in the same assay. Thus, compound **8** was slightly weaker than DIC. It must be emphasized that none of the hit molecules have been optimized yet, and there existed a possibility for improving the binding affinity of each compound after careful molecular optimization. Therefore, the discovery of the new scaffolds with relatively good potency was encouraging. The IC_{50} curves of DIC and the representative compounds **8** and **13** were shown in Fig. 8.

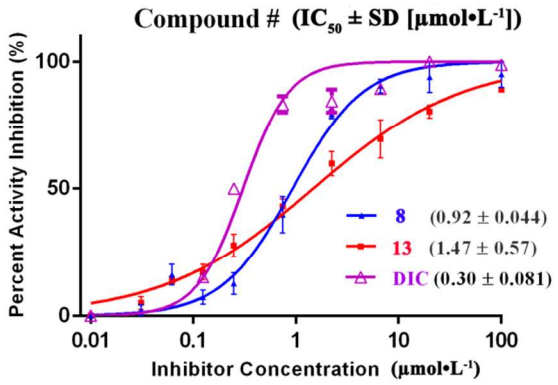

Fig. 8 The IC_{50} curves of DIC and the representative compounds **8** and **13**.

In order to obtain the possible binding mode of NQO1 with these inhibitors, a molecular docking study was performed using the crystal structure of NQO1. The docking poses of the representative compounds **8**, **10** and **13** were shown in Fig. 9. The general molecular orientation and the spatial location of the chemical features of these inhibitors were similar to that of DIC (Fig. 9). The planner ring makes π-stacking interaction with the isoalloxazine ring of the bound cofactor FAD, and the side chains of these compounds could fit into the additional pocket formed by Tyr128, Phe232 and Phe236. The well occupied

pose of these compounds indicated that they were potential inhibitors of NQO1.

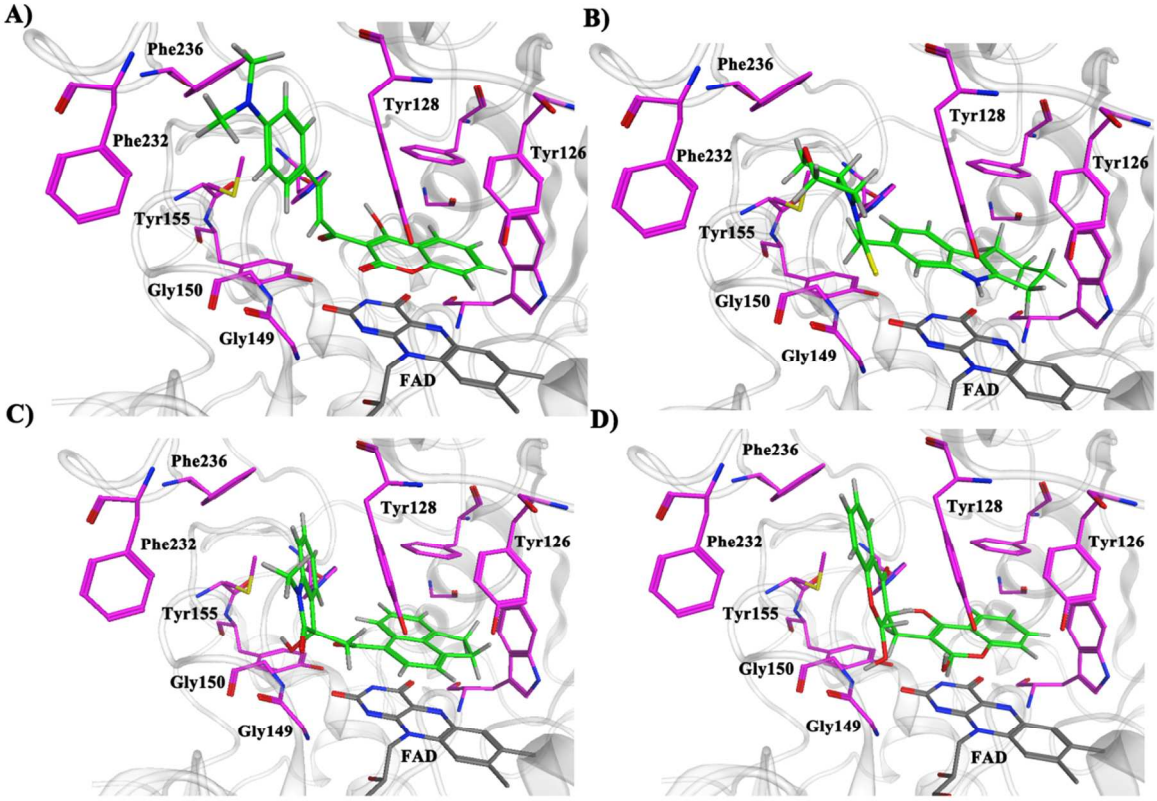

Fig. 9 The docking-predicted binding mode of **8**, **10**, **13** and crystal binding mode of DIC. (A, B, C, D) **8**, **10**, **13** and DIC in the active site of NQO1 respectively, key residues were labelled in stick.

The main goal for developing NQO1 inhibitors was to use these compounds as tool or probe for better understanding the pharmacological function of NQO1. Therefore, compounds with little to no cytotoxic effects are required. A549 (NQO1-rich) cells were first treated for 48 h with 50 μmol•L^{-1} of these inhibitors to determine their cytotoxicity. Three of the inhibitors (**8**, **10** and **13**) showed non-toxic towards A549 cells (data not shown). Afterwards, for the purpose of measuring the pharmacological efficiency of these compounds to act as inhibitors of NQO1 in cells, a surrogate method was used according to the reference.[30] The ability to inhibit the toxicity of β-lap can be regarded as a measure of the pharmacological efficiency of these compounds to act as inhibitors of NQO1 in cells. A549 cells were then treated with various concentrations of β-lap and 30 μmol•L^{-1} of the compounds. In previous work, we have tested the IC_{50} of β-lap for A549 cells.[6,31] The inhibitor should elicit a decrease in toxicity of β-lap (A549, IC_{50} = 4.5 ± 0.9 μmol•L^{-1}). Fig. 10 showed the dose response curves for A549 cells incubate with β-lap and the NQO1 inhibitors **8**, **10** and **13**. Coincubation with **8**, **10** and **13** protects A549 cells from β-lap-mediated cell death, shifting the IC_{50} 4-fold to 8-fold. The fold is the ratio of the IC_{50} in the present with β-lap and inhibitor to the IC_{50} of treatment with only β-lap. The higher ratio indicates greater protection for these NQO1 inhibitors. All of these three compounds appeared to be potent compound for protecting against β-lap toxicity in A549 cells and the ability for protecting against the toxic effects of β-lap was comparable to that of the positive control DIC (shifting the IC_{50} 6-fold). The results were shown in Fig. 10 and indicated that these compounds are efficient NQO1 inhibitors which can be employed as tool for better understanding the pharmacological function of NQO1.

Journal Name RSCPublishing

ARTICLE

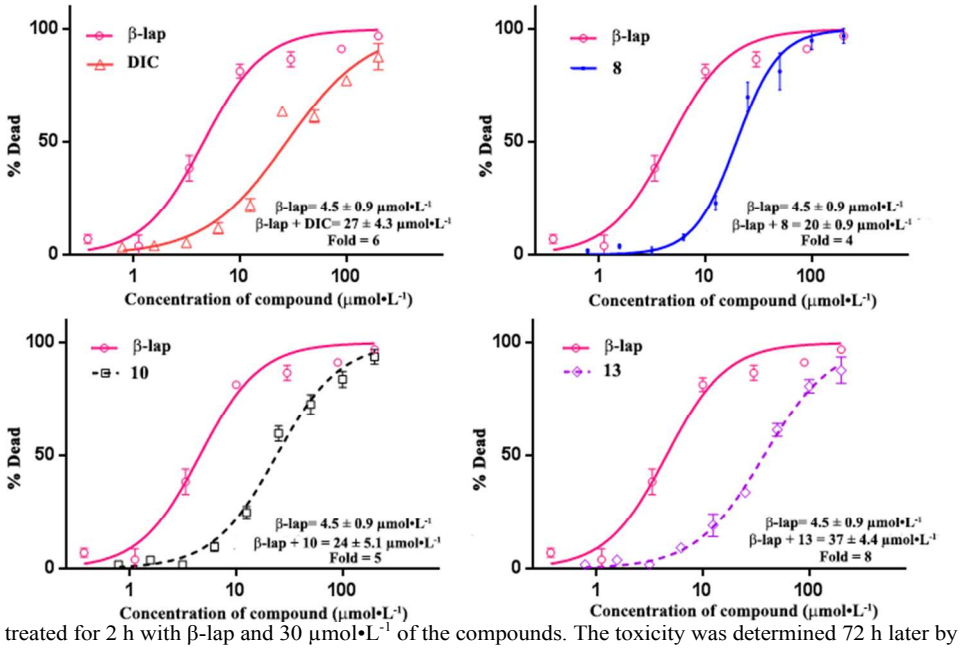

Fig. 10 A549 cells were treated for 2 h with β-lap and 30 μmol•L^{-1} of the compounds. The toxicity was determined 72 h later by the MTT assay.

4. Conclusions

With the combined strategy of similarity search and molecular docking study, a diverse range of scaffolds of NQO1 inhibitors were identified from the ChemDiv database. The shape-based screening model was built using the ROCS method, based on DIC and ES936, two recognized inhibitors of NQO1. Cascade docking was used to ensure that the protein, the docking program and evaluation were optimal for this docking process with NQO1. Testing the 43 hit compounds has led to several submicromolar inhibitors with similar potency to NQO1 competitive inhibitor DIC. The main goal of this work is to obtain agents which many be pharmacological useful for studying NQO1. Thus, taking advantage of the fact that tumor cells A549 expressing high levels of functional NQO1 are sensitive to β-lap, these inhibitors were determined for their ability to be functional in cells. Among them, compounds **8**, **10** and **13** (**DDO-5203, DDO-5205 and DDO-5208**) showed the ability for protecting against the toxic effects of β-lap, which was comparable to that of the positive control DIC. In this direction the virtual screen approach showed can also be used to screen existing database to identify derivatives with desired activity. Further studies on the molecular optimization of the other hits to provide some other potent NQO1 inhibitors with novel scaffolds are currently underway.

Acknowledgements

We are thankful for the financial support of the National Natural Science Foundation of China (No.81302636), the Natural Science Foundation of Jiangsu Province of China (No.BK20130656), the Program of State Key Laboratory of Natural Medicines, China Pharmaceutical University (No.SKLNMZZ201202), the National Found for Fostering Talents of Basic Science (NFFTBS) of China (No. J1030830), the Priority Academic Program Development of Jiangsu Higher Education Institutions (PAPD).

Notes and references

[a] Jiangsu Key Laboratory of Drug Design and Optimization, China Pharmaceutical University, Nanjing, 210009, China

[b] State Key Laboratory of Natural Medicines, China Pharmaceutical University, Nanjing, 210009, China

[c] Department of Medicinal Chemistry, School of Pharmacy, China Pharmaceutical University, Nanjing, 210009, China

[d] Department of Organic Chemistry, School of Science, China Pharmaceutical University, Nanjing, 210009, China

* Corresponding authors. Tel/fax: +86 2583271351 (Q. Y.); tel: +86 2583271216 (X. Z.). E-mail: wang_yalou@tom.com (Y. Wang); youqd@163.com (Q. You), zxj@cpu.edu.cn (X. Zhang)

† Electronic Supplementary Information (ESI) available: [details of any supplementary information available should be included here]. See DOI: 10.1039/b000000x/

References

1 D. Siegel, D. L. Gustafson, D. L. Dehn, J. Y. Han, P. Boonchoong, L. J. Berliner, D. Ross, *Mol. Pharmacol.*, 2004, **65**, 1238-1247.

2 K. Liao, F. Niu, H. P. Hao, G. J. Wang, *Chin. J. Nat. Med.*, 2012, **10**, 170–176.

3 M. Faig, M.A. Bianchet, P. Talalay, S. Chen, S. Winski, D. Ross, L.M. Amzel, *Proc. Natl. Acad. Sci. U. S. A.*, 2000, **97**, 3177-3182.

4 M. Faig, M.A. Bianchet, S. Winski, R. Hargreaves, C. J. Moody, A. R. Hudnott, L. M. Amzel, *Structure*, 2001, **9**, 659-667.
5 S. L. Winski, M. Faig, M. A. Bianchet, D. Siegel, E. Swann, K. Fung, M.W. Duncan, C. J. Moody, L. M. Amzel, D. Ross, *Biochemistry*, 2001, **40,** 15135-15142.
6 J. Bian, B. Deng, L. Xu, X. Xu, N. Wang, T. Hu, Z. Yao, J. Du, L. Yang, H. Sun, X. Zhang, Q. You, *Eur. J. Med. Chem.*, 2014, **82**, 56-67.
7 D. Ross, J. K. Kepa, S. L. Winski, H.D. Beall, A. Anwar, D. Seigel, *Chem-Biol. Interact.*, 2000, **129**, 77–97.
8 (a) M. A. Colucci, P. Reigan, D. Siegel, A. Chilloux, D. Ross, C. J. Moody, *J. Med. Chem.*, 2007, **50**, 5780-5789. (b) K. W. Wellington, *RSC Adv.* 2015, **5**, 20309-20338.
9 G. Asher, N. Reuven, Y. Shaul, Bioessays, 2006, **28**, 844-849.
10 K. A. Nolan, M. P. Humphries, J. Barnes, J. R. Doncaster, M. C. Caraher, N. Tirelli, R. A. Bryce, R. C. Whitehead, I. J. Stratford, *Bioorg. Med. Chem.*, 2010, **18**, 696-706.
11 A. Alard, B. Fabre, R. Anesia, C. Marboeuf, P. Pierre, C. Susini, C. Bousquet, S. Pyronnet, *Mol Cell Biol.*, 2010, **30**, 1097-1105.
12 P. Tsvetkov, G. Asher, V. Reiss, Y. Shaul, L. Sachs, J. Lotern, *Proc. Natl. Acad. Sci. U. S. A.*, 2005, **102**, 5535-5540.
13 S. L. Winski, E. Swann, R. H. J. Hargreaves, D. L. Dehn, J. Butler, C.J. Moody, D. Ross, *Biochem. Pharmacol.*, 2001, **61**, 1509-1516.
14 E. I. Parkinson, J. S. Bair, M. Cismesia, P. J. Hergenrother, *ACS Chem. Biol.*, 2013, **8**, 2173-2183.
15 F. Liu, G. Yu, G. Wang, H. Liu, X. Wu, Q. Wang, M. Liu, K. Liao, M. Wu, X. Cheng, H. Hao, *PloS One*, 2012, **7**, e42138.
16 K. A. Nolan, D. J. Timson, I. J. Stratford, R. A. Bryce, *Bioorg. Med. Chem. Lett.*, 2006, **11**, 6246-6254.
17 K. A. Nolan, H. Zhao, P. F. Faulder, A. D. Frenkel, D. J. Timson, D. Siegel, D. Ross, T. R. Burke Jr, I. J. Stratford, R. A. Bryce, *J. Med. Chem.*, 2007, **50**, 6316-6325.
18 K. A. Nolan, J. R. Doncaster, M. S. Dunstan, K. A. Scott, A. D. Frenkel, D. Siegel, R. A. Bryce, *J. Med. Chem.*, 2009, **52**, 7142-7156.
19 ROCS, version 3.1.2.; OpenEye Scientific Software: Santa Fe, NM, 2013.
20 ChemDiv. 2015. http://www.chemdiv.com.
21 Chemical computing group releases MOE version 2013.08.
22 T. S. Rush, J. A. Grant, L. Mosyak, A. Nicholls, *J. Med. Chem.*, 2005, **48**, 1489−1495.
23 K. Moffat, V. J. Gillet, M. Whittle, G. Bravi, A. R. Leach, *J. Chem. Inf. Model.*, 2008, **48**, 719−729.
24 J. E. Fuchs, G. M. Spitzer, A. Javed, A. Biela, C. Kreutz, B. Wellenzohn, K. R. Liedl, *J. Chem. Inf. Model.*, 2011, **51**, 2223-2232.
25 J. Kirchmair, P. Markt, S. Distinto, G. Wolber, T. Langer, *J. Comput.-Aided Mol. Des.*, 2008, **22**, 213–228.
26 N. Triballeau, F. Acher, I. Brabet, J.P. Pin, H.O. Bertrand, *J. Med. Chem.*, 2005, **48**, 2534–2547.
27 R. Thilagavathi, R. L. Mancera, *J. Chem. Inf. Model.*, 2010, **50**, 415−421.
28 H. P. Sun, J. M. Jia, F. Jiang, X. L. Xu, F. Liu, X. K. Guo, B. Cherfaoui, H. Z. Huang, Y. Pan, Q. D. You, *Eur. J. Med. Chem.*, 2014, **79**, 399-412.
29 R. Li, M. A. Bianchet, P. Talalay, L. M. Amzel, *Proc. Natl. Acad. Sci. U. S. A.*, 1995, **92**, 8846−8850.
30 K. A. Nolan, K. A. Scott, J. Barnes, J. Doncaster, R. C. Whitehead, I. J. Stratford, *Biochem. Pharmacol.*, 2010, **80**, 977-981.
31 J. Bian, L. Xu, B. Deng, X. Qian, J. Fan, X. Yang, F. Liu, X. Xu, X. Guo, X. Li, H. Sun, Q. You, X. Zhang, *Bioorg. Med. Chem. Lett.*, 2015, **25**, 1244-1248.